Assessing Reorganisation of Functional Connectivity in the Infant Brain

Roxane Licandro[1,2], Karl-Heinz Nenning[2], Ernst Schwartz[2],
Kathrin Kollndorfer[2], Lisa Bartha-Doering[3], Hesheng Liu[4], Georg Langs[2]
`licandro@caa.tuwien.ac.at`

[1]Institute of Computer Aided Automation - Computer Vision Lab, Vienna University of Technology; [2]Department of Biomedical Imaging and Image-guided Therapy - Computational Imaging Research Lab, Medical University of Vienna; [3]Department of Pediatrics and Adolescent Medicine, Medical University of Vienna; [4]Department of Radiology, Martinos Center, MGH, Harvard Medical School

Abstract. As maturation of neural networks continues throughout childhood, brain lesions insulting immature networks have different impact on brain function than lesions obtained after full network maturation. Thus, longitudinal studies and analysis of spatial and temporal brain signal correlations are a key component to get a deeper understanding of individual maturation processes, their interaction and their link to cognition. Here, we assess the connectivity pattern deviation of developing resting state networks after ischaemic stroke of children between 7 and 17 years. We propose a method to derive a reorganisational score to detect target regions for overtaking affected functional regions within a stroke location. The evaluation is performed using rs-fMRI data of 16 control subjects and 16 stroke patients. The developing functional connectivity affected by ischaemic stroke exhibits significant differences to the control cohort. This suggests an influence of stroke location and developmental stage on regenerating processes and the reorganisational patterns.

1 Introduction

Human brain development starts during pregnancy and proceeds in building structural as well as functional trajectories through adulthood until senescence [17]. Morphological, functional, and cognitive maturation is shaped by genetic and environmental influence such as learning processes and experience after birth, and the resulting structure varies substantially across individuals [21]. While the functional and morphological organization of the adults brain is known to a large extent, we are only starting to understand its emergence and maturation [17]. We know that we can observe distributed components similar to those in adults already in neonates [8], while substantial changes to the brain network structure occur during childhood, such as an increase in long-, and a decrease in short-distance connections from infants to adults [5]. However, these observations primarily focus on the comparison of age snapshots, and do not capture multivariate temporal change patterns of the connectome. There is a particularly critical gap in knowledge concerning normal development confronted with disease or adverse events such as stroke.

Paediatric Ischaemic Stroke (IS) is caused by a decreased blood flow in cerebral vessels (ischaemia), which in an irreversible case leads to the death of brain cells and forming of brain lesions [15]. Stroke in children is a rare event, with an international incidence of 1.2 to 13 per 100,000 children per year under 18 years of age [19]. Children, who survive an IS, suffer from lifelong motoric or cognitive disabilities as well as developing or learning problems. Their outcome varies over age, the stroke location or additional comorbidities [15]. Functional MRI techniques (fMRI) enable the measurement of functional organisation [4]. In comparison to task-based fMRI, pediatric resting state (rs)fMRI aims to image neural activation and analyse brain signals due to their temporal correlation independent of a stimulus [1] in a non-invasive way.

Plasticity is the process which enables the central nervous system to dynamically adapt to external stimuli. Natural plasticity is induced by the age and developmental related changes of the brain and is triggered by learning and experience [2], where adaptive plasticity refers to pathology related modifications, e.g. functional an structural reorganisation of brain tissue after stroke [13]. Also genetic factors can drive these processes [12]. While we have gained some understanding in reorganization processes in adults [14], we have poor understanding of how reorganization interacts with development. Resting state fMRI enables the study of these processes driving the functional and structural organisation. Ultimately they can lead to improved functional outcome of children suffering from brain injuries, by developing novel interventional techniques or adapting therapy, dependent on the developmental stage of a disease [13].

Challenges The challenges for studying reorganisation in children lies in capturing the dynamics of interactions between adaptive and developmental processes. After a damage, plasticity and vulnerability of the brain influence recovery together with the injuries severity, the age and the time since damage [2]. Functional recovery after brain injury depends on the ability of the brain to adapt to changes [9]. Recent studies suggest that cognitive abilities after brain injury is dependent on the plasticity of neural networks that control brain functions [10]. Thus, the impact of brain injury on cognition is best studied by investigating neuronal networks rather than circumscribed areas [3]. As maturation of neural networks continues throughout childhood [5], brain lesions insulting immature networks have a different impact on function than lesions acquired after full network maturation. A deeper understanding of individual continuous maturation processes, their interaction, and their link to cognition is essential for our understanding of the functional brain architecture, treatment and optimal promotion of children [12].

Contribution The methodological contribution of this work is two-fold: (1) we propose a technique to quantify connectivity pattern deviation in the development of functional connectivity, and (2) a method to *track* regions which exhibit similar connectivity characteristics as *source* regions such as an area impacted by stroke after reorganization. We hypothesize that (1) stroke subjects exhibit

higher deviation from a control population age specific mean than controls, and (2) reorganization causes new regions to adopt connectivity characteristics of areas impaired by stroke due to reorganization. We adapt an approach by [16] to extract connectivity pattern deviation over development and reorganisational patterns of functional connectivity in children induced by laesions forming after an ischaemic stroke. The methodologies proposed are summarised in Section 2. The evaluation setup and computed results are documented in Section 3 and a discussion and possibilities for future work are given in Section 4.

2 Methodology

In this section the methodology is introduced, by providing (1) a Connectivity Profile Deviation (CPD) score to analyse deviations between control and stroke subjects and (2) by tracking reorganization using the the proposed prior. For the formulations we assume a graph based representation of the cortical surface, which is previously normalized to a standardized surface consisting of nodes $x = 1 \ldots N$. For every subject the Connectivity Matrix $CM \in \mathbb{R}^{N \times N}$ is computed and stroke masks are annotated (for more details regarding the preprocessing and dataset used cf. Section 3).

Age specific reference of connectivity profiles across the cortex According to the size of the dataset and preliminary analysis we decided to perform element wise linear regression of correlation coefficient matrices of control subjects to derive the slope $B \in \mathbb{R}^{N \times N}$. An age matched correlation matrix $\overline{CM}$ is then computed using Equation 1.

$$\overline{CM}^{age} = B * age + B_0 \tag{1}$$

Identifying deviations of local connectivity characteristics In a second step the CPD score $D \in \mathbb{R}^{1 \times N}$ is computed between every single subject's CM^s and the age matched $\overline{CM}^{age_s}$ using Pearson Correlation Coefficient (PCC) (cf. Equation 2).

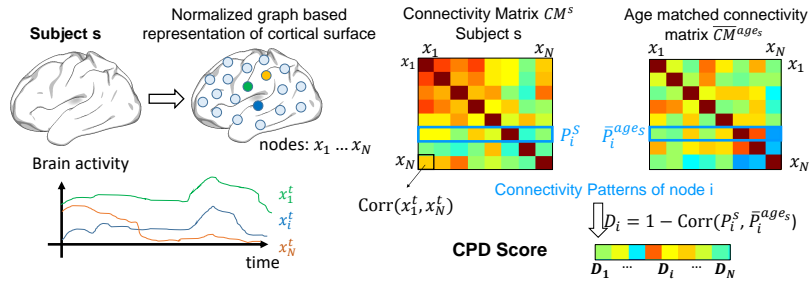$$D_x^s = 1 - PCC(P_x^s, \overline{P}_x^{age_s}), x = 1 \ldots N \tag{2}$$

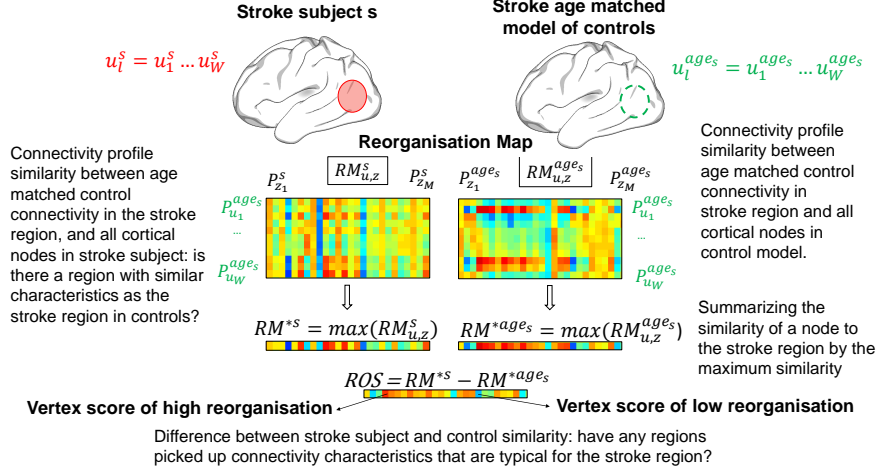Fig. 1: Schematic illustration of the computation of the CPD score.

Fig. 2: Schematic illustration of the computation of the reorganisation score.

Therefore, a connectivity pattern $P_x^s \in \mathbb{R}^{1 \times N}$ of a vertex x and the corresponding age matched connectivity pattern $\overline{P}_x^{age_s} \in \mathbb{R}^{1 \times N}$ of controls are computed, where $P_x^s = CM_{i=x,j}$, $\overline{P}_x^{age_s} = \overline{CM}_{i=x,j}^{age_s}$, $j = 1 \ldots N$ (cf. Fig. 1).This CPD score is computed for every subject s in the dataset (control and stroke cases).

Finding target areas of reorganization In this work we propose a *ReOrganisation Score (ROS)* for identifying possible regions, where functional networks of a stroke region transfer to. For clearer understanding its computation is schematically illustrated in Fig. 2. In a first step the corresponding stroke case's age matched $\overline{CM}^{age}$ is computed. In a second step for every stroke subject separately the stroke mask is used to determine the set $u, 1 \ldots W, W \leq N$ of nodes corresponding to the stroke regions. In a third step we compute the Reorganisation Maps (RM) $RM_{u,z}^s$ and $RM_{u,z}^{age_s}$ between connectivity patterns using Equation 3 and 4. We define $z = x \setminus u$ as set of nodes not belonging to the stroke region. $\overline{P}_{u_l}^{age_s} = \overline{CM}_{i=u_l,j=z}^{age_s}$, $P_{z_k}^s = CM_{i=z_k,j=z}$, $\overline{P}_{z_k}^{age_s} = \overline{CM}_{i=z_k,j=z}$, $k = 1 \ldots M, M = | x \setminus u |, l = 1 \ldots W$.

$$RM_{u,z}^s = PCC(\overline{P}_u^{age_s}, P_{z_k}^s), s = 1 \ldots S \tag{3}$$

$$RM_{u,z}^{age_s} = PCC(\overline{P}_u^{age_s}, \overline{P}_{z_k}^{age_s}), s = 1 \ldots S \tag{4}$$

After the calculation of the RMs we extracted the vertex of set u with the maximum value. Since RM of the control model show higher values as RM of the stroke, we decided (for obtaining comparability for visualisation purposes) to perform histogram equalisation, resulting in two vectors $RM^{*s} \in \mathbb{R}^{1 \times M}$ and $RM^{*age_s} \in \mathbb{R}^{1 \times M}$. Subsequently, we estimate the ROS of a subject S as defined in Equation 5.

$$ROS = RM^{*s} - RM^{*age_s}, \tag{5}$$

Table 1: Participant demographics

	Control	Pediatric stroke
Sample size	16 (7 female)	16 (5 female)
Excluded	4	5
Mean age, yr (Standard Deviation)	11.2 (3.19)	11.63 (3.14)
Stroke location (number of subjects)	-	RH (7), LH (7), RH+LH (2)

3 Results

The participants in this study are 32 children between 7 and 17 years consisting of 16 control cases and 16 ischaemic stroke cases (cf. participant demographics in Table 1). Subject No.15 (control), No.17 (stroke), and No.21 (stroke) were excluded, due to technical issues during acquisition. During the preprocessing phase three stroke Subjects (No.3, 10 and 22) and control Subjects (No.26, 33 and 34) were excluded because of high motion artefacts (5 subjects) and severe stroke (more than the half of the size of a hemisphere was affected). The stroke events occurred at different spatial locations on the right (RH) or left hemisphere (LH). The children were right-, left- or mixed handed. The time frame between scan event and stroke event, as well as the range of the age at stroke of the children ranges from 0 to 15 years. All participants' guardians (parents) were informed about the aim of the study and gave their written, informed consent prior to inclusion. The protocol of this study was approved by the national ethics committee of the Medical University of Vienna and performed in accordance with the Declaration of Helsinki (1964), including current revisions and the EC-GCP guidelines. The scanning was performed on a 3T TIM Trio System (Siemens Medical Solution, Erlangen, Germany) Scanner and rs-fMRI measurements were performed using single-shot, gradient-recalled, echo-planar imaging with the following setup: TR = 2000 ms, TE = 42 ms, FOV = 210 x 210mm, slices = 20, gap between slices = 1 mm, slice thickness = 4 mm, frames = 150 volumes. All subjects are scanned in an awake state with open eyes for 5 minutes. To restrict head motion, pillows are used as fixation on both sides of the child's head. The probands wore headphones to attenuate the noise level during scan. All study participants watched a video, explicitly designed for children, which showed and explained an MRI acquisition procedure.

Anatomical and Functional Preprocessing Anatomical and functional preprocessing is performed using Freesurfer[1][6] and FSL[2][11]. The functional preprocessing includes a registration to the anatomical data, head motion regression and bandpass temporal filtering (0.01 - 0.1 Hz) to remove constant offsets and linear trends. Cerebral signals of the stroke and control cases are resampled to common FreeSurfer fsaverage5 space [7]. After this alignment every subject's cortical surface is represented as a standardized mesh consisting of 20484 nodes.

---

[1] `http://surfer.nmr.mgh.harvard.edu` [accessed 16th May 2017]
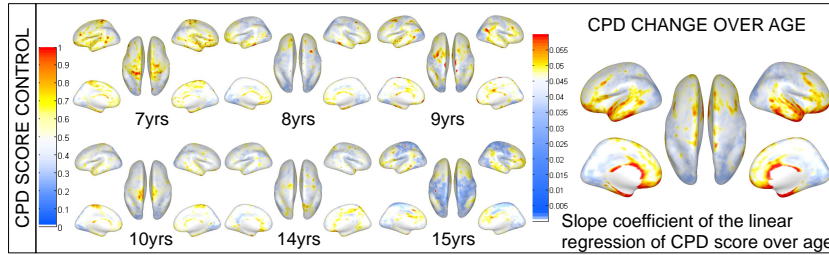[2] `http://fsl.fmrib.ox.ac.uk/fsl/fslwiki/FSL` [accessed 16th May 2017]

Fig. 3: Visualisation of the CPD score in control subjects during ageing: 6 control subjects and their deviation to the age matched average, and the visualisation of the change: red regions exhibit increased deviation / deviation change, while blue regions are more stable.
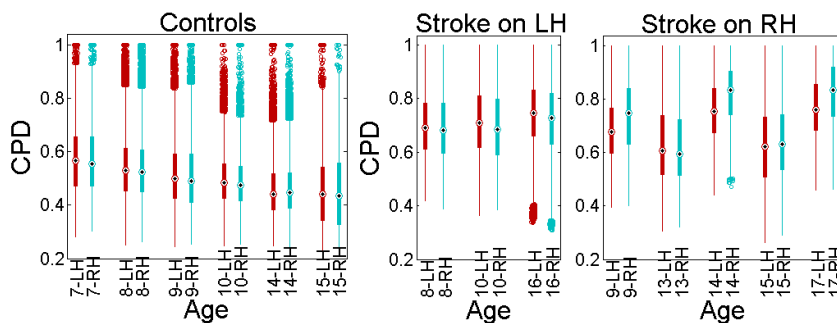

Fig. 4: Visualisation of CPD score of LH and RH within the stroke and control cohort (CPD scores of all subjects at same age are grouped here). Control cases show symmetric mean CPD between RH and LH and a decrease according to increasing age. The CPD scores of stroke subjects show higher means on the hemisphere of stroke location.

After resampling the data are spatially smoothed using a 4 mm FWHM Gaussian filter. For the identification of correlating regions, the PCC is computed between the time course of a node $x(t)_i$ in each subject's brain and every other node's $x(t)_j$ time course. This results in a correlation coefficient matrix $CM_{i,j} \in \mathbb{R}^{N \times N}$, where N is the number of nodes observed, $i = 1 \ldots N$ the ith row and $j = 1 \ldots N$ the jth column of the matrix [18]. For every subject in the stroke cohort masks of brain lesion are annotated by an expert and also preprocessed using the introduced preprocessing pipeline.

Deviation of local connectivity characteristics in the control cohort
Fig. 3 illustrates the CPD score for control subjects of different age (left) and its change over increasing age (right). The intersubject deviation of controls is minimal in the visual, sensory and motor cortices and correlates with increasing age to the deviation estimates in [16] of adult controls. High deviation is observed
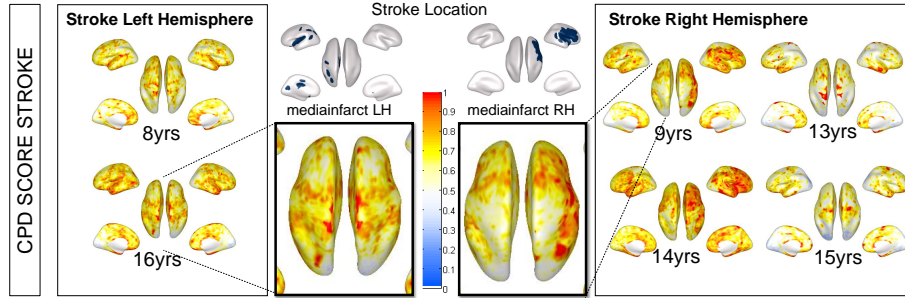
Fig. 5: Visualisation of CPD score of LH stroke subjects (left) and RH stroke subjects (right).

in the temporal cortex including primary auditory cortex, Wernicke's area, in the prefrontal cortex and parietal lobe. Considering the age a decrease of deviation in the heteromodal regions is observable with increasing age also visible in the corresponding boxplot of CPD scores in Fig. 4 (left).

Deviation of local connectivity characteristics in the stroke cohort For the stroke subjects RH and LH stroke cases are grouped together for clearer visualisation in Fig. 5. The stroke cohort shows higher variabilities compared to the control cohort, which overlaps with the hypothesis that stroke effects the reorganisation of connectivity networks, resulting in higher CPD. It is observable that higher intersubject CPD over 0.8 are observable on the hemisphere of stroke location also visible in the corresponding boxplot of CPD scores in Fig. 4 (middle, right).

Target regions of reorganisational processes To evaluate the ability of the ROS to detect reorganisational regions we first devided the brain surface into 17 cortical networks using the parcellation proposed by Yeo et al. [20], which is computed based on rsfMRI acquisitions of 1000 subjects and additionally provides fsaverage 5 surface labels. For every region (total 36 - LH and RH are observed separately) the ratio of stroke voxels and the region's mean ROS and mean CPD are estimated. In Fig. 6 the first row illustrates correlation matrices $\in \mathbb{R}^{36 \times 36}$ based on correlations computed between the ratio of stroke voxels and mean CPD for all subjects (first column), for LH stroke subjects (second column) and RH stroke subjects (third column). In Fig. 6 second row the mean ROS score is used instead of the mean CPD to estimate the correlations. In Fig. 6 a deviation of correlation values between LH and RH stroke subjects is visible, since correlations only between a stroke voxel ratio ($>$0) on the ipsilateral side can be computed. In the first row of Fig. 6 positive correlations are observable, which can be interpreted as regions greater affected by a stroke lesion show a higher mean CPD and a lower mean CPD if they are less affected. Additionally, stronger blocks of correlation scores are observable in the default mode network regions (except the temporal component Default A) or somato motoric areas. In
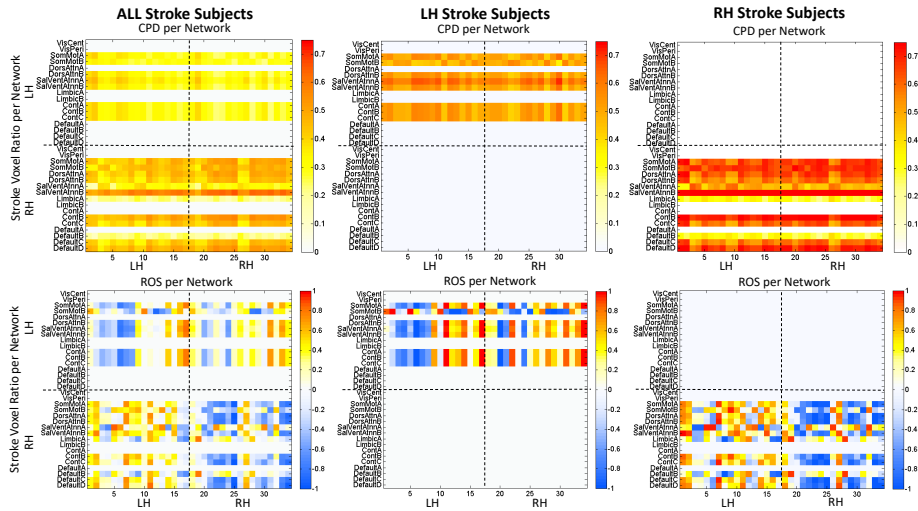
Fig. 6: Row one visualises the network wise correlations between the stroke voxel ratio and the CPD score using all stroke subjects (first column), LH stroke (second column) and RH stroke subjects (third column). Visualisation of network wise correlations between the stroke voxel ratio and the ROS are shown in row two.

the second row of Fig. 6 especially for RH stroke subjects (right) a division of RH and LH correlation values according to their sign is visible, since the severity of stroke and number of subjects is higher in this cohort compared to LH stroke subjects. The voxel ratio positively correlates with the ROS of the controlateral side and negatively with the ROS of the ipsilateral side. This suggests a decrease of the ROS in ipsilateral and an increase of the ROS in controlateral regions with increased stroke voxel ratio in the stroke hemisphere. In Fig. 7 the target regions for possible reorganisational processes after stroke, computed using the ROS proposed are visualised for LH stroke subjects (left) and RH stroke subjects (right). The first row visualises the stroke location, the second row the ROS and the third and fourth row the histogram equalized reorganisation vectors. Subject S08 shows possible target regions in its strokes neighbourhood on the ipsilateral side. S11 shows possible symmetric reorganisation targets. S13 and S23 with a severe mediainfarct on the RH show both on the contro and ipsilateral side of non-stroke region an increased ROS as well as on the controlateral side in the stroke region.

4 Conclusion

We present a methodology to assess connectivity pattern deviation in developing functional networks and to estimate possible target regions of reorganisational processes after ischaemic stroke. According to the results we can conclude that
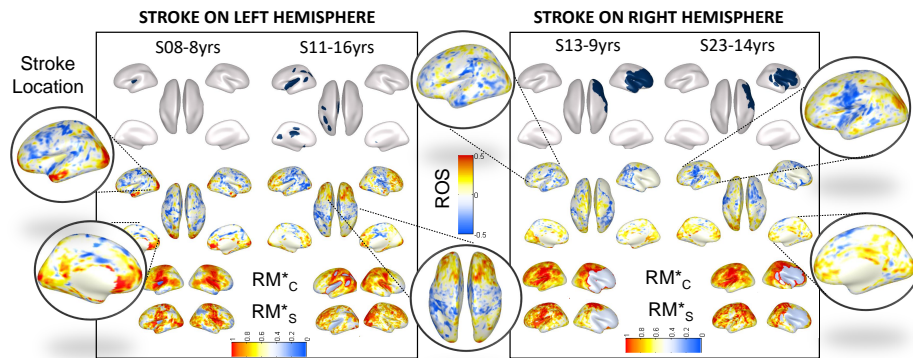
Fig. 7: Visualisation of regions that pick up connectivity patterns observed in the stroke region in age matched control average. Red ROS indicates regions that exhibit characteristics typical for the stroke regions if the subject is a control.

stroke subjects show a higher deviation compared to control subjects, especially more on the hemisphere of stroke location. Control subjects show decreasing deviation over age to age matched controls, with highest changes occuring in the prefrontal cortex and temporal lobe. We proposed a reorganisational score, which identifies ipsi-lateral and symmetric networks in neighbourhood of the stroke location as possible indicator for reorganisation in developing resting state networks. The limit of our approach lies in the size and heterogeneity of the dataset. For future work we will evaluate different stroke datasets with similar locations of the stroke lesions and a higher number of participants.

Acknowledgement

References

1. N.R. Altman and B. Bernal. Clinical applications of functional magnetic resonance imaging. *Pediatric Radiology*, 45(3):382–396, 2015.
2. V. Anderson, M. Spencer-Smith, and A. Wood. Do children really recover better? Neurobehavioural plasticity after early brain insult. *Brain : a journal of neurology*, 134(Pt 8):2197–221, 2011.
3. E. Bullmore and O. Sporns. Complex brain networks: graph theoretical analysis of structural and functional systems. *Nature Reviews Neuroscience*, 10(3):186–198, 2009.
4. B. Casey, N. Tottenham, C. Liston, and S. Durston. Imaging the developing brain: what have we learned about cognitive development? *TiCS*, 9(3):104–110, 2005.

5. D.A. Fair, A.L. Cohen, J.D. Power, N.U.F. Dosenbach, J.A. Church, F.M. Miezin, B.L. Schlaggar, and S.E. Petersen. Functional brain networks develop from a "local to distributed" organization. *PLoS computational biology*, 5(5):e1000381, 2009.

6. B. Fischl. FreeSurfer. *Neuroimage*, 62(2):774–81, August 2012.

7. B. Fischl, M.I. Sereno, R.B. Tootell, and A.M. Dale. High-resolution intersubject averaging and a coordinate system for the cortical surface. *Human brain mapping*, 8(4):272–84, 1999.

8. W. Gao, H. Zhu, K.S. Giovanello, J. K. Smith, D. Shen, J.H. Gilmore, and W. Lin. Evidence on the emergence of the brain's default network from 2-week-old to 2-year-old healthy pediatric subjects. *P.N.A.S. of the U. S. A.*, 106(16):6790–5, 2009.

9. P.R. Huttenlocher. *Neural plasticity : the effects of environment on the development of the cerebral cortex*. Harvard University Press, 2002.

10. T. Ius, E. Angelini, M. Thiebaut de Schotten, E. Mandonnet, and H. Duffau. Evidence for potentials and limitations of brain plasticity using an atlas of functional resectability of WHO grade II gliomas: Towards a minimal common brain. *NeuroImage*, 56(3):992–1000, 2011.

11. M. Jenkinson, C.F. Beckmann, T.E.J. Behrens, M.W. Woolrich, and S.M. Smith. FSL. *NeuroImage*, 62(2):782–90, aug 2012.

12. M.V. Johnston. Plasticity in the developing brain: Implications for rehabilitation. *Developmental Disabilities Research Reviews*, 15(2):94–101, 2009.

13. S. Kornfeld, J.A. Delgado Rodríguez, R. Everts, A. Kaelin-Lang, R. Wiest, C. Weisstanner, P. Mordasini, M. Steinlin, and S. Grunt. Cortical reorganisation of cerebral networks after childhood stroke:impact on outcome. *BMC Neurology*, 15(1):90, 2015.

14. V. La Corte, M. Sperduti, C. Malherbe, F. Vialatte, S. Lion, T. Gallarda, C. Oppenheim, and P. Piolino. Cognitive Decline and Reorganization of Functional Connectivity in Healthy Aging: The Pivotal Role of the Salience Network in the Prediction of Age and Cognitive Performances. *Front. in Aging Neuroscience*, 8:204, 2016.

15. J.K. Lynch, D.O., M.P. H., C.J. Han, and B. A. Pediatric Stroke - What Do We Know and What Do We Need to Know? *Sem. in Neurology*, 25(4):410–423, 2005.

16. S. Mueller, D. Wang, M.D. Fox, B.T.T. Yeo, J. Sepulcre, M.R. Sabuncu, R. Shafee, J. Lu, and H. Liu. Individual Variability in Functional Connectivity Architecture of the Human Brain. *Neuron*, 77(3):586–595, 2013.

17. J. D. Power, D.A. Fair, B.L. Schlaggar, and S.E Petersen. The development of human functional brain networks. *Neuron*, 67(5):735–48, sep 2010.

18. J. Sepulcre, H. Liu, T. Talukdar, I. Martincorena, B.T. Thomas Yeo, and R.L. Buckner. The organization of local and distant functional connectivity in the human brain. *PLoS Computational Biology*, 6(6):1–15, 2010.

19. D.S. Tsze and J.H. Valente. Pediatric stroke: a review. *Emergency medicine international*, 2011:734506, 2011.

20. B.T.T. Yeo, F.M. Krienen, J. Sepulcre, M.R. Sabuncu, D. Lashkari, M. Hollinshead, J.L. Roffman, J.W. Smoller, L. Zöllei, J.R. Polimeni, B. Fischl, H. Liu, and R.L. Buckner. The organization of the human cerebral cortex estimated by intrinsic functional connectivity. *Journal of neurophysiology*, 106(3):1125–65, sep 2011.

21. K. Zilles, N. Palomero-Gallagher, and K. Amunts. Development of cortical folding during evolution and ontogeny. *Trends in Neurosciences*, 36(5):275–284, 2013.